Magnetization reversal and nanostructure refinement in magnetically annealed $Nd_2Fe_{14}B/\alpha$-Fe-type nanocomposites

B. Z. Cui[a)]
National High Magnetic Field Laboratory, Florida State University, Tallahassee, Florida 32310

C. T. Yu
Department of Physics, Miami University, Oxford, Ohio 45056

K. Han
National High Magnetic Field Laboratory, Florida State University, Tallahassee, Florida 32310

J. P. Liu
Department of Physics, University of Texas at Arlington, Arlington, Texas 76019

H. Garmestani
School of Materials Science and Engineering, Georgia Institute of Technology, Atlanta, Georgia 30332

M. J. Pechan
Department of Physics, Miami University, Oxford, Ohio 45056

H. J. Schneider-Muntau
National High Magnetic Field Laboratory, Florida State University, Tallahassee, Florida 32310

(Presented on 8 November 2004; published online 10 May 2005)

Nanostructure refinement, magnetic anisotropy and hard magnetic property enhancement have been observed in melt-spun $Nd_{2.4}Pr_{5.6}Dy_1Fe_{84}Mo_1B_6$ nanocomposites annealed in an in-plane or out-of-plane field of 1.2 T. The magnetic annealing results in an enhancement of an out-of-plane (110) crystal texture of α-Fe and an in-plane uniaxial magnetic anisotropy of the 2:14:1 phase. Magnetic annealing also introduces finer, less angular and more homogeneously distributed soft and hard nanograins. Field dependent torque measurement indicates a complex magnetization reversal mechanism in these nanocomposites. Compared with the sample annealed without a field, there is a noticeable improvement in the hard magnetic properties for the magnetically annealed samples. Especially, the energy product $(BH)_{max}$ was enhanced by 26.6% (from 94 to 119 kJ/m^3). The improvement in the magnetic properties is a result of the enhanced crystallographic texture, nanostructure refinement, and in-plane uniaxial magnetic anisotropy enhancement. © *2005 American Institute of Physics*. [DOI: 10.1063/1.1853693]

Homogenized and textured nanostructures are essential for the achievement of record-high $(BH)_{max}$ in nanocomposites.[1–3] This paper reports a study of magnetization reversal, crystallographic texture, nanostructure refinement, magnetic anisotropy enhancement, and further hard magnetic property improvement in melt-spun $Nd_{2.4}Pr_{5.6}Dy_1Fe_{84}Mo_1B_6$ nanocomposites annealed with and without a field of 1.2 T.

$Nd_{2.4}Pr_{5.6}Dy_1Fe_{84}Mo_1B_6$ ribbons were prepared by melt spinning with a molybdenum wheel speed of 35 m/s. The ribbons from the same melt-spun run were annealed at 680 °C for 1 min in the same furnace (a) without a field, (b) with a 1.2 T in-plane field (1.2 T, //), i.e., the field is parallel to the transverse direction of the ribbon plane, and (c) with a 1.2 T out-of-plane field (1.2 T, $\perp$), i.e., the field is perpendicular to the ribbon plane.

Phases and crystallographic textures, nanostructure and crystallization of the samples were studied by XRD, TEM, and DSC at a heating rate of 20 °C/min, respectively. Magnetic torqueses were measured in fields up to 9 T at 250 K with a torque magnetometer. The room-temperature magnetic properties of ribbons were measured by a SQUID magnetometer in fields up to 7 T.

XRD investigations demonstrate that the as-spun alloy is composed of a mixture in which a small amount of α-Fe and $(Nd,Pr,Dy)_2(Fe,Mo)_{14}B$ (2:14:1) nanocrystallines are embedded in an soft amorphous matrix. Annealing at 680 °C for 1 min leads to the formation of a composite of α-Fe and 2:14:1 phases. The intensity of (220) reflection is notably greater than those of (211) and (200) reflections (see Fig. 1 and the inset). The I_{220}/I_{211} values of α-Fe are 1.2, 1.9, and 2.5 for the samples (a), (b), and (c), respectively, where I_{220} and I_{211} are the integrated intensities of (220) and (211) reflection peaks. Those values are higher than 0.33 for the random α-Fe powder, obtained from JCPDS 6-0696. This suggests that there is an out-of-plane (110) crystal texture of α-Fe in the annealed ribbons. It should be noted that, the α-Fe in the as-spun alloy is already partially textured with I_{220}/I_{211} of 0.57. Here XRD was done on the free side of all the ribbons. There is no noticeable texture difference in the free and wheel sides of the annealed overquenched ribbons.

The average grain sizes of α-Fe, calculated from the (110) diffractions using the Scherrer formula, are 16 nm and 19 nm (with error bar of 10%) for the samples annealed with

[a)]Author to whom correspondence should be addressed. Tel: 850-645-1241; Fax: 850-644-0867; electronic mail: bcui@magnet.fsu.edu

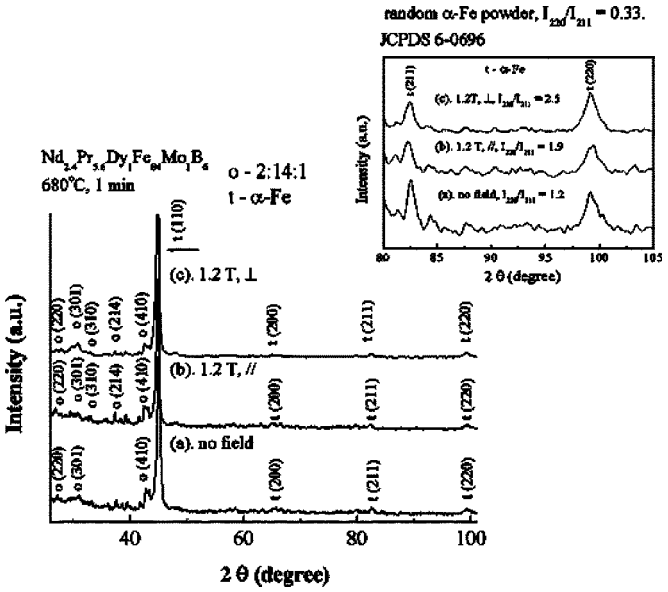

FIG. 1. XRD patterns of $Nd_{2.4}Pr_{5.6}Dy_1Fe_{84}Mo_1B_6$ ribbons annealed at 680 °C for 1 min (a) without a field, (b) with a 1.2 T in-plane field (||), (c) with a 1.2 T out-of-plane field ($\perp$). The inset is an enlarged part of 2θ =80-105°.

and without a field, respectively. TEM results shown in Fig. 2 confirmed the x-ray results. Magnetic annealing introduces somewhat finer, less angular, and more homogeneously distributed soft and hard nanograins.

DSC study shows that nucleation temperatures of the α-Fe and 2:14:1 phases are 525 °C and 590 °C, respectively. The growth of the (110) texture of α-Fe in the sample annealed without a field may be attributed to a seeding effect of the texture in the as-spun alloy, formed during the melt-spinning process due to directional solidification under a thermal gradient.[4,5] The magnetic anneal temperature in this work (680 °C) is lower than the Curie temperature of α-Fe (771 °C). In the magnetic crystallization process, the drive force due to magnetocrystalline anisotropy energy of α-Fe

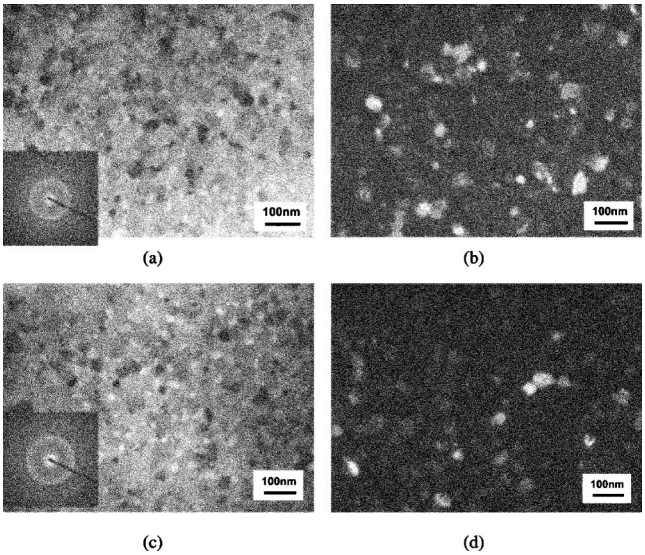

FIG. 2. TEM bright and dark field images, and corresponding selected area diffractions of $Nd_{2.4}Pr_{5.6}Dy_1Fe_{84}Mo_1B_6$ ribbons annealed at 680 °C for 1 min (a–b) without a field, (c–d) with a 1.2 T out-of-plane field.

that is still in a ferromagnetic state could be larger than those due to the energy associated with the shape anisotropy and the thermal disordering effect, which may induce a magnetic-phase-textured nanostructure.[6] The seeding effect of the texture in the as-spun alloy and the magnetocrystalline anisotropy of α-Fe are suggested be the reasons for the enhancement of (110) texture of α-Fe in the samples annealed with a field. On the other hand, the prealigned α-Fe grain seeds may induce hard phase with somewhat preferred crystallographic orientation as a result of defined habit plane for nucleation and orientation relationship between the hard and soft phases.[5] It is believed that some planes of the 2:14:1 phase, such as (301) and (310), can grow epitaxially from the (110) plane of α-Fe due to a small lattice mismatch.[5] As shown in Fig. 1, an enhancement of intensity of (301) reflection is indeed observed in the sample (c).

The presence of a field results in an increase of the driving force for crystallization of α-Fe due to its ferromagnetic magnetocrystalline anisotropy, and further, increases the nucleation rate of α-Fe.[7] So, compared with the annealing without a field, the magnetic annealing leads to reduced α-Fe grain sizes and more uniform distribution of the hard and soft nanograins. In addition, magnetic annealing should have a similar but much weaker effect on increase of the nucleation rate of the 2:14:1 phase due to its paramagnetic state during the crystallization process.

In-plane magnetic anisotropy of the annealed ribbons was evaluated by magnetic torque measurements. The magnetic field is applied in the ribbon plane, and the sample rotates forward in the field from 0° to 360° and then backward to 0°. All samples demonstrate typical uniaxial torque curves. To extract the anisotropy constant, the experimental data were fit with an equation derived from uniaxial anisotropy in a saturation field of 9 T.[8] The obtained anisotropy constant K_1 is 3.5×10^4, 6.3×10^4, and 7.0×10^4 J/m^3 for the samples (a), (b), and (c), respectively. It is noteworthy that the magnetic annealing results in a noticeable enhancement of the in-plane uniaxial anisotropy, which is the consequence of the crystallographic textures discussed above.

Field dependent torque curves have also been measured, in an attempt to understand the magnetization reversal mechanism of the nanocomposite system. The inset of Fig. 3 shows the typical torque curves at different external fields. The extracted rotational hysteresis loss, which is defined as the net work required to rotate the sample through 360° in a fixed magnetic field and often assists in determining the reversal mechanism, is also plotted in Fig. 3 for all three samples. At low field, the torque is unidirectional in nature, indicating that the net moment moves only slightly from its easy axis during rotation of the field, which arises from the strong intergrain exchange coupling. At 9 T, the moment is continually aligned with the field revealing the uniaxial anisotropy discussed above. At all values between the lowest and largest applied fields the forward and reverse torque curves are separated, with a large positive bias for the forward and negative bias for the reverse torque. This phenomena has been observed[8–10] in composite films with strong internal magnetostatic interactions, and been labeled "rotatable easy axis" or "rotatable initial susceptibilities,"[9,10]

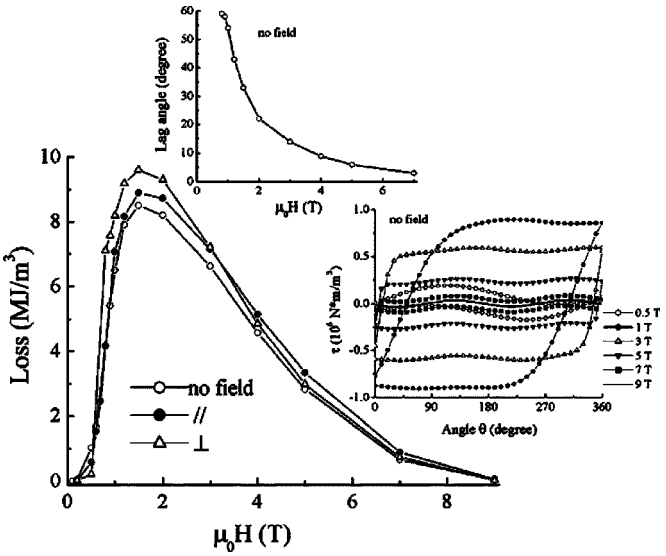

FIG. 3. Field-dependent rotational-hysteresis loss of the three samples of Fig. 1. The insets are magnetization lag angle vs applied field curve and rotational-hysteresis curves of the sample annealed without a field, respectively. θ is angle between the magnetic field and the transverse direction of the ribbon plane.

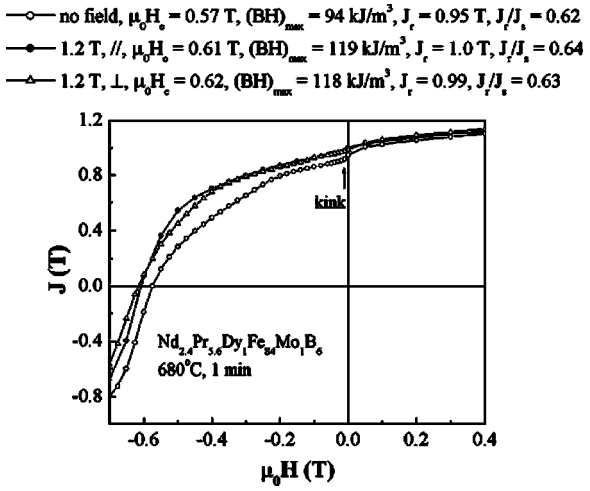

FIG. 4. Half hysteresis loops of the three samples of Fig. 1.

though the details of the underlying mechanism were not fully modeled. The superposition of a small amplitude torque signal with these large offsets reflects the presence of two magnetic anisotropies—one rotatable and one fixed. The rotatable likely arises from the randomly distributed magnetic entities (the hard nanocomponents in our case), which exerts a constant torque, on average, when the sample rotates in a field that is sufficiently large to induce, but not fully saturate the magnetization in the hard magnets. During rotation, this induced moment lags the applied field direction, with maximum lag angle inversely related to the field strength. In fact, this maximum lag angle at a given field can be directly obtained from the data as the torque zero-crossing angle upon reversal (see the inset of Fig. 3). Although quite intriguing, further elaboration on this phenomena remains beyond the scope of this paper. It can be seen that the samples with magnetic annealing possess larger rotational hysteresis loss than the one annealed without field. This implies the intergrain coupling in the nanocomposites has been enhanced due to their structural refinements.

Figure 4 shows half hysteresis loops of the three samples of Fig. 1 and the corresponding magnetic properties. Compared with the sample (a), magnetically annealed samples demonstrate an improvement in intrinsic coercivity $\mu_0 H_c$, remanence J_r, reduced remanence J_r/J_s and energy product $(BH)_{max}$. After the magnetic annealing, the kink at the demagnetization curves disappeared and additionally, a better squareness of the demagnetization curves was observed. The field directions seem to have little effect on the magnetic properties in our case. This may be due to texture of the 2:14:1 phase is still not strong, which is field-direction-dependent.[11] The improvement in the magnetic properties is a comprehensive result of the crystallographic textures, magnetic-field-induced in-plane uniaxial anisotropy enhancement and especially, an enhanced exchange coupling due to nanostructural refinements (such as, crystallite size and shape, distribution of the magnetic grains, and defect density, etc.).[11]

This work was supported by DARPA through ARO under Grant No. DAAD19-03-1-0038 and US DOE (MU).

[1] A. Manaf, R. A. Buckley, and H. A. Davies, J. Magn. Magn. Mater. **128**, 302 (1993).
[2] B. Z. Cui, X. K. Sun, L. Y. Xiong, W. Liu, Z. D. Zhang, Z. Q. Yang, A. M. Wang, and J. N. Deng, J. Mater. Res. **16**, 709 (2001).
[3] R. Skomski and J. M. D. Coey, Phys. Rev. B **48**, 15812 (1993).
[4] M. J. Kramer, L. H. Lewis, L. M. Fabietti, Y. Tang, W. Miller, K. W. Dennis, and R. W. McCallum, J. Magn. Magn. Mater. **241**, 144 (2002).
[5] X. Y. Zhang, Y. Guan, L. Yang, and J. W. Zhang, Appl. Phys. Lett. **79**, 2426 (2001).
[6] P. Courtois, R. P. de la Bâthie, and R. Tournier, J. Magn. Magn. Mater. **153**, 224 (1996).
[7] C. J. Yang and E. B. Park, IEEE Trans. Magn. **32**, 4428 (1996).
[8] M. Prutton, *Thin Ferromagnetic Films* (Butterworths, Washington, 1964).
[9] M. S. Cohen, J. Appl. Phys. **33**, 2968 (1962).
[10] J. M. Lommel and C. D. Graham, J. Appl. Phys. **33**, 1160S (1962).
[11] B. Z. Cui, *et al.* (to be published).